Influences of high-temperature annealing on atomic layer deposited Al_2O_3/4H-SiC*

Wang Yi-Yu(王弋宇)[a], Shen Hua-Jun(申华军)[a]†, Bai Yun(白 云)[a], Tang Yi-Dan(汤益丹)[a], Liu Ke-An(刘可安)[b], Li Cheng-Zhan(李诚瞻)[b], and Liu Xin-Yu(刘新宇)[a]

[a] *Department of Microwave Devices and Integrated Circuits, Institute of Microelectronics, Chinese Academy of Sciences, Beijing* 100029, *China*
[b] *Zhuzhou CSR Times Electric Co. Ltd., Zhuzhou* 412001, *China*

(Received 7 November 2012; revised manuscript received 31 January 2013)

High-temperature annealing of the atomic layer deposition (ALD) of Al_2O_3 films on 4H-SiC in O_2 atmosphere is studied with temperature ranging from 800 °C to 1000 °C. It is observed that the surface morphology of Al_2O_3 films annealed at 800 °C and 900 °C is pretty good, while the surface of the sample annealed at 1000 °C becomes bumpy. Grazing incidence X-ray diffraction (GIXRD) measurements demonstrate that the as-grown films are amorphous and begin to crystallize at 900 °C. Furthermore, *C*–*V* measurements exhibit improved interface characterization after annealing, especially for samples annealed at 900 °C and 1000 °C. It is indicated that high-temperature annealing in O_2 atmosphere can improve the interface of Al_2O_3/SiC and annealing at 900 °C would be an optimum condition for surface morphology, dielectric quality, and interface states.

Keywords: Al_2O_3, SiC, high-temperature annealing, crystallize

PACS: 81.40.Ef, 73.20.–r, 73.40.Qv **DOI:** 10.1088/1674-1056/22/7/078102

1. Introduction

Investigation of high-*k* dielectrics on SiC, such as Al_2O_3,[1–3] HfO_2,[4] and AlN[5] has recently attracted great interest due to reliability issue of SiC MOSFETs,[6,7] which derives from the high density of shallow interface states below the conduction band edge E_c and the relatively low dielectric constant of SiO_2 ($\varepsilon \sim 3.9$) compared with that of 4H-SiC ($\varepsilon \sim 9.7$). Al_2O_3 is attractive as an alternative gate dielectric because it simultaneously presents a large dielectric constant ($\varepsilon \sim 10$) and a large band gap (∼6.2 eV) in comparison with other high-*k* materials.[8] However, Al_2O_3 films have different microstructures and chemical natures from those of SiC substrates. Therefore, the interface properties of as-grown Al_2O_3/SiC are not as good as expected due to the high density of trap charges existing at the interface and in the bulk oxide.[9] Several studies have demonstrated that interface quality and electrical properties for atomic layer deposition (ALD) Al_2O_3/SiC devices could be partly improved after annealing in Ar or N_2 ambient at 1000 °C.[10,11] However, the flatband voltage is still as high as 6 V, and large effective charges (10^{13} cm^{-2}) remain at the interface. It is noted that Al_2O_3 films deposited by atomic layer deposition are usually amorphous and oxygen deficient.[12] The oxygen vacancies were examined to be the most important defects in ALD Al_2O_3, and they may induce gap levels introducing border traps near the interface.[13] Therefore, in order to further reduce the high density of trap charges, annealing in O_2 atmosphere might be an effective way to further reduce the defects in ALD Al_2O_3 films and improve the interface quality of Al_2O_3/SiC.

In this study, Al_2O_3 gate oxide layers are deposited by ALD on 4H-SiC at 300 °C, and then annealed at temperature ranging from 800 °C to 1000 °C in O_2 atmosphere. Surface morphology is characterized through scanning electron microscopy (SEM) and atomic force microscope (AFM) measurements. The changes in film thickness and optical constants are evaluated with SE measurements. Grazing incidence X-ray diffraction (GIXRD) analyses were performed to investigate the microstructural characteristics. Electrical properties are characterized by *C*–*V* measurements. Results demonstrate that Al_2O_3/SiC annealed at 900 °C has attractive characteristics of good surface morphology, small positive flat-band voltage shift, and a very small hysteresis.

2. Experimental setup

N-type, 4 °C off (0001) oriented, 4H-SiC wafers with 12.76-μm-thick epilayer doped with nitrogen (5.16×10^{15} cm^{-3}) were used. The wafers were cleaned by following the conventional Radio Corporation of America (RCA) clean procedure, and then dipped into a diluted hydrofluoric acid solution to remove native oxide from the SiC surface. The Al_2O_3 films were deposited using the ALD technique with trimethylaminium (TMA) and water as precursors at a reactor temperature of 300 °C. The thickness of Al_2O_3 films was obtained to be 20 nm by SE measurements. Post deposition annealing

*Project supported by the National Natural Science Foundation of China (Grant No. 61106080) and the Major Program of the National Natural Science Foundation of China (Grant No. 2013ZX02305).

†Corresponding author. E-mail: shenhuajun@ime.ac.cn

© 2013 Chinese Physical Society and IOP Publishing Ltd

treatments have been carried out in oxygen atmosphere from 800 °C to 1000 °C for 30 min. Besides, to evaluate the influences on the electrical properties of films, MIS-capacitor test structures were also fabricated on all the samples for *C*–*V* measurements. The pads were patterned to a circular shape with a diameter of 0.2 mm. Then, 20-nm/200-nm Ni/Au layers were deposited by e-beam evaporation, followed by a lift-off process. A 150-nm Ni layer was used for the ohmic contact at the back side.

The SE measurements were performed on a UVISEL spectroscopic ellipsometer. The triple-angle method with incident angles of 65 °C, 70 °C, and 75 °C was used to characterize the refractive index n and thickness of Al_2O_3 films. The Cauchy model was chosen for fitting the dispersive optical constants to the ellipsometric data for transparent Al_2O_3 films.[14] The morphologies of the as-grown and annealed Al_2O_3 films were compared by using SEM and AFM. The effect of the annealing on structural modifications was investigated by GIXRD with an incidence angle of 1 °C. Then, the *C*–*V* measurements were conducted on the MIS capacitors by using an Agilent 4284A precision impedance analyzer. All the measurements were implemented at room temperature.

3. Results and discussion

AFM images of the surface morphology of as-grown and annealed Al_2O_3 films are shown in Fig. 1. It can be seen in Fig. 1(a) that the as-deposited Al_2O_3 film has excellent step coverage and thickness uniformity. The root mean square (RMS) roughness of the as-grown film surface is only about 0.91 nm, indicating that the ALD method is very suitable for the growth of high-k materials which require excellent conformity and large-area uniformity. Figures 1(b)–1(d) show the AFM morphologies of annealed samples at different temperatures. The grain size increases and the uniformity deteriorates after high-temperature annealing. The plot of RMS value versus annealing temperature is shown in Fig. 1(e). The RMS roughness of as-grown Al_2O_3 and annealed samples (at 800,

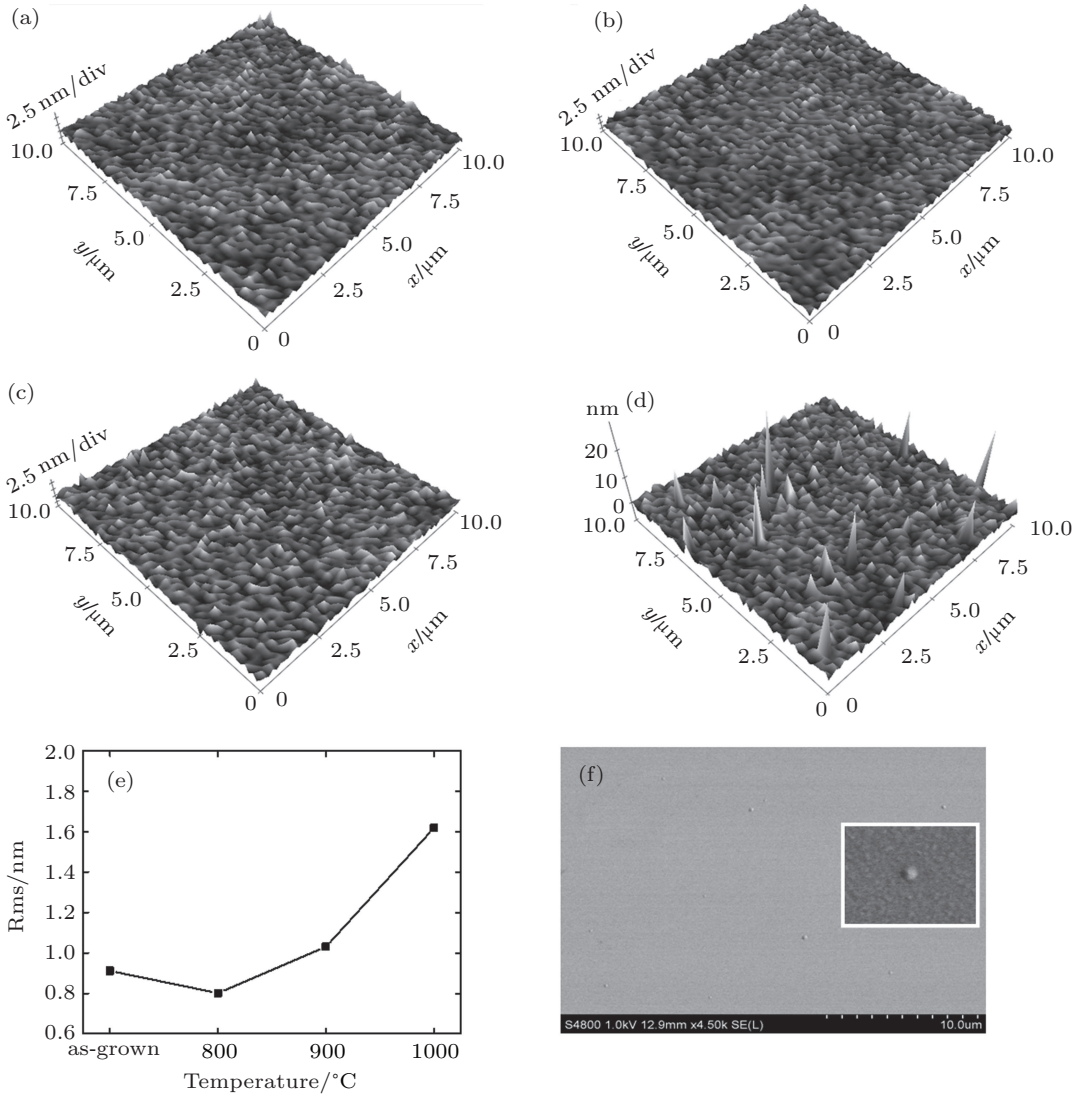


Fig. 1. AFM images of (a) as-grown Al_2O_3 film, and ALD-Al_2O_3 films annealed at (b) 800 °C, (c) 900 °C, (d) 1000 °C. (e) Plot of the RMS value versus the annealing temperature. (f) SEM image of Al_2O_3 film annealed at 1000 °C, and the inset shows the enlarged image of the bubble.

900, and 1000 °C) are 0.911, 0.801, 1.031, and 1.619 nm, respectively. The RMS tends to increase with increasing annealing temperature. The increase in surface roughness may enhance scattering, and reduce the channel mobility.[15] When annealing temperature reaches 1000 °C, bubble formation occurs on the surface of Al_2O_3 film, as shown in Fig. 1(d). The SEM images of the bubbles are shown in Fig. 1(f). It should be pointed out that thick Al_2O_3 films have also been deposited and annealed, but the blistering is aggravated. We infer that blistering is probably partial de-lamination of a thick Al_2O_3 layer caused by gaseous desorption in the Al_2O_3 layer upon thermal treatments above a critical temperature.[16] Hence, both the thickness of films and the annealing temperature influence the deterioration of dielectric film.

The changes in the film thickness and the optical constants after O_2 annealing were evaluated with SE measurements. The fitted film thickness and refractive index n as functions of annealing temperature obtained from the Al_2O_3 film on SiC substrate are shown in Fig. 2. The fitted Al_2O_3 film thickness for as-grown sample and annealed samples at 800, 900, and 1000 °C are 19.3, 17.0, 18.8, and 20.3 nm, respectively. For the sample annealed at 800 °C, the decrease in the thickness indicates a densification of the loosely arranged as-deposited film. When the annealing temperature increases, oxygen may be incorporated to the Al_2O_3 film, resulting in an increase in its thickness. This result is consistent with that reported in Ref. [17]. As shown in Fig. 2, the refractive index n of the annealed Al_2O_3 films at the wavelength of 633 nm also shows an obvious increase with increasing annealing temperature. This may be associated with the crystallization of the ALD Al_2O_3 films during annealing because different structures of the samples influence the optical properties greatly.[18]

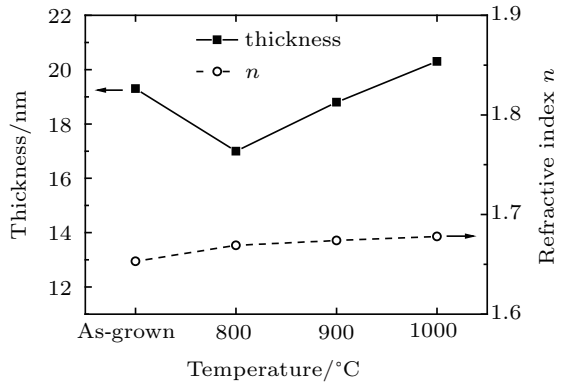


Fig. 2. Thickness measured by spectroscopic ellipsometry versus annealing temperature for ALD-Al_2O_3, and the refractive indices for Al_2O_3 films at the wavelength of 633 nm versus annealing temperature.

Figure 3 shows the GIXD spectra of as-grown Al_2O_3 film and Al_2O_3 films annealed at various temperatures. Peaks are not observed in the as-grown Al_2O_3 film and the film annealed at 800 °C, indicating that they are amorphous. In the case of Al_2O_3 films annealed at 900 °C, the (440) diffraction peak of γ-Al_2O_3 appears at an angle of $2\theta \approx 66.5$ °C, meaning a transition from amorphous phase to crystalline phase. It is known that polycrystalline dielectrics usually have larger leakage currents than amorphous films due to the leakage through domain boundaries. Comparing the Al_2O_3 films annealed at 900 °C and 1000 °C, we find that the peak intensity increases and the full width at half maximum (FWHM) of the diffraction peak decreases as the annealing temperature increases. Hence, Al_2O_3 film crystallization has been improved by increasing the annealing temperature. It confirms the conclusion about the refractive index n. The above results indicate that the as-deposited films are amorphous and begin to crystallize at 900 °C.

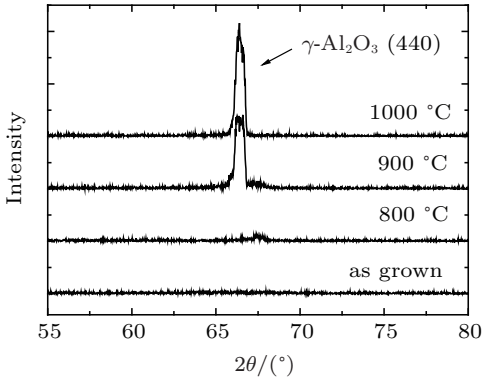


Fig. 3. Grazing incidence X-ray diffraction patterns for the ALD Al_2O_3 annealed at different temperatures.

High-frequency (1 MHz) C–V measurements have been performed on as-grown and annealed Al_2O_3/SiC capacitors sweeping from depletion to accumulation, and then backwards. For the as-grown Al_2O_3/SiC capacitors, a very low breakdown voltage was found to prevent the capacitors from reaching full accumulation. Normalized typical C–V curves for annealed Al_2O_3/SiC capacitors are shown in Fig. 4. The flatband voltage shift (ΔV_{fb}) is found by comparing the experimental and theoretical results. An estimation of the effective charge density (Q_{eff}) has also been obtained from ΔV_{fb}. The hysteresis voltage ($\Delta V_h = V_{fb_inv_to_acc} - V_{fb_acc_to_inv}$) is defined as the difference between the extracted flatband voltage (V_{fb}) corresponding to the two voltage sweeps. The electrical parameters extracted from C–V curves including measured V_{fb}, ΔV_{fb}, ΔV_h, and Q_{eff}, are summarized in Table 1. The Al_2O_3/SiC capacitor annealed at 800 °C shows a relatively large ΔV_{fb} (3.477 V) and ΔV_h (2.865 V). However, for the samples annealed at 900 °C and 1000 °C, ΔV_{fb} equals 1.780 and 1.734 V, respectively. In the two cases, ΔV_h are negligible and the effective charge densities are also less than half of that of the sample annealed at 800 °C. Furthermore, interface states density (D_{it}) is estimated by the Terman method. The D_{it} close to the conductance band edge of Al_2O_3/SiC capacitors annealed at 800, 900, and 1000 °C are 4.7×10^{12},

0.80×10^{12}, and 0.81×10^{12} $eV^{-1} \cdot cm^{-2}$, respectively. Moreover, the capacitor annealed at 800 °C has the highest value of D_{it}. In order to compare the D_{it} of capacitors annealed at 900 °C and 1000 °C, mean values from measurements of five different capacitors are used. The D_{it} close to the conductance band edge of samples annealed at 900 °C and 1000 °C, are 0.82×10^{12} and 0.85×10^{12} $eV^{-1} \cdot cm^{-2}$, respectively, which are comparative. Because the Al_2O_3/SiC capacitors annealed at 900 °C and 1000 °C show better electrical characterizations and it has been proved by GIXRD results that the as-deposited Al_2O_3 films begin to crystallize at 900 °C, we conclude that this improvement may be correlated with the crystallization of Al_2O_3 layers and the re-formation of Al_2O_3/SiC interfaces. Thus, the negative effective charges located at near interfaces and in bulk oxides have been reduced significantly after high-temperature annealing.

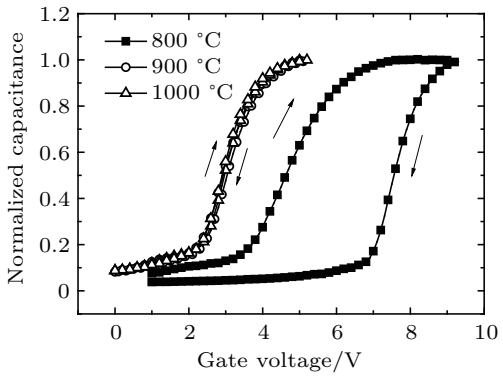


Fig. 4. Normalized typical high-frequency (1 MHz) *C–V* curves for annealed MIS capacitors. The gate voltage sweeping direction is indicated by arrows.

Table 1. List of measured V_{fb}, ΔV_{fb}, hysteresis voltage (ΔV_h), and effective oxide charge (Q_{eff}) for Al_2O_3/SiC MIS capacitors.

	800 °C	900 °C	1000 °C
Measured V_{fb}/V	4.785	3.088	3.042
ΔV_{fb}/V	3.477	1.780	1.734
ΔV_h/V	2.865	0.100	0.060
Q_{eff} /10^{12} cm^{-2}	−2.871	−1.316	−1.283

4. Conclusions

We have investigated the effect of high-temperature annealing on 4H-SiC MIS capacitors with an Al_2O_3 gate dielectric prepared by the ALD method. Blistering occurs on the surface of the Al_2O_3 film when the annealing temperature reaches 1000 °C, indicating the deterioration of the dielectric film. SE measurements demonstrated that the thickness increased as the annealing temperature increased. The as-deposited Al_2O_3 films were amorphous and begun to crystallize at 900 °C. The *C–V* measurements exhibit that the flatband voltage and hysteresis voltage of Al_2O_3/SiC capacitors annealed at 900 °C and 1000 °C have been reduced significantly. Thus, the annealing temperature of 900 °C is an optimal annealing temperature for improving the bulk properties of the Al_2O_3 film and the interface of Al_2O_3/SiC.

References

[1] Lazar H R, Misra V, Johnson R S and Lucovsky G 2001 *Appl. Phys. Lett.* **79** 973

[2] Liu L, Yang Y T and Ma X Y 2011 *Chin. Phys. B* **20** 127204

[3] Tang X Y, Song Q W, Zhang Y M, Zhang Y M, Jia R X, Lü H L and Wang Y H 2012 *Chin. Phys. B* **21** 087701

[4] Taube A, Gieraltowskac S, Gutta T, Malachowskia T, Pasternaka I, Wojciechowskic T, Rzodkiewicza W, Sawickic M and Piotrowska A 2011 *Acta Phys. Pol. A* **119** 696

[5] Komatsu N, Satoh T, Honjo M, Futatuki T, Masumoto K, Kimura C and Aoki H 2011 *Appl. Surf. Sci.* **257** 8307

[6] Singh R 2006 *Microelectron Reliab.* **46** 713

[7] Song Q W, Zhang Y M, Han J S, Philip T, Sima D, Zhang Y M, Tang X Y and Guo H 2013 *Chin. Phys. B* **22** 027302

[8] Groner M D, Elam J W, Fabreguette H H and George S M 2002 *Thin Solid Films* **413** 186

[9] Avice M, Grossner U, Pintilie I, Svensson B G, Servidori M, Nipoti R, Nilsen O and Fjellvag H 2007 *J. Appl. Phys.* **102** 054513

[10] Avice M, Grossner U, Nilsen O, Christensen J S, Fjellvag H and Svensson B G 2006 *Phys. Scr.* **126** 9

[11] Avice M, Grossner U, Nilsen O, Christensen J S, Fjellvag H and Svensson B G 2006 *Mater. Sci. Forum.* **527** 1067

[12] Perevalov T V, Tereshenko O E, Gritsenko V A, Pustovarov V A, Yelisseyev A P, Park C, Han J H and Lee C 2010 *J. Appl. Phys.* **108** 013501

[13] Weber J R, Janotti A and van de Walle C G 2011 *J. Appl. Phys.* **109** 033715

[14] Petrik P, Szilagyi E, Lohner T, Battistig B, Fried M, Dobrik G and Biro L P 2009 *J. Appl. Phys.* **106** 123506

[15] Saito S, Hisamoto D, Kimura S and Hiratani M 2003 *International Electron Devices Meeting Technical Digest,* December 8, 2003 Washinton DC, American, p. 797

[16] Vermang B, Goverde H, Lorenz A, Uruena A, Vereecke G, Meersschaut J, Cornagliotti E, Rothschild A, John J, Poortmans J and Mertens R 2011 *37th IEEE Photovoltaic Specialists Conference,* June 19, 2011 Seattle, America, p. 3562

[17] Correa S A, Marmitt G G, Bom N M, Rosa A T, Stedile F C, Radtke C, Soares G V, Baumvol I J R, Krug C and Gobbi A L 2009 *Appl. Phys. Lett.* **95** 051916

[18] Zhu Y Y, Fang Z B and Xu R 2011 *J. Rare Earth.* **29** 958